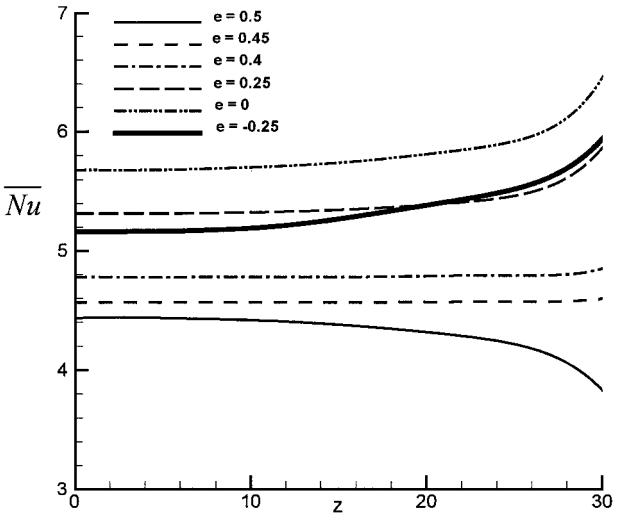

Fig. 5 Axial distributions of the averaged Nusselt number on the inner cylinder for the six examined configurations.

Figure 5 compares the averaged Nusselt number distributions on the cable surfaces of the six examined configurations. Here the averaged Nusselt number is defined by

$$\overline{Nu}(z) = \frac{1}{\pi}\int_0^{\pi} Nu(\phi, z)\,\mathrm{d}\phi \tag{4}$$

where

$$Nu(\phi, z) = 1/[\theta_w(\phi, z) - \theta_b(z)] \tag{5}$$

Note that the Nusselt number defined on the outer (concrete conduit) surface is identically zero due to the specified adiabatic boundary condition. Except for the case of $e = 0.5$, the Nusselt number $\overline{Nu}$ for the other five cases increase toward the open end.

Acknowledgment

The authors gratefully acknowledge grant support from the National Science Council, Republic of China, under Contract NSC89-2213-E-150-007.

References

[1] Yeh, C. L., and Chang, K. C., "Natural Convection Simulation Inside the Underground Conduit of an Electrical Power Cable," *Journal of Thermophysics and Heat Transfer*, Vol. 14, No. 4, 2000, pp. 557–565.

[2] Kuehn, T. H., and Goldstein, R. J., "An Experimental Study of Natural Convection Heat Transfer in Concentric and Eccentric Horizontal Cylindrical Annuli," *Journal of Heat Transfer*, Vol. 100, No. 4, 1978, pp. 635–640.

[3] Prusa, J., and Yao, L. S., "Natural Convection Heat Transfer Between Eccentric Horizontal Cylinders," *Journal of Heat Transfer*, Vol. 105, No. 1, 1983, pp. 108–116.

[4] Ho, C. J., and Lin, Y. H., "Natural Convection Heat Transfer of Cold Water Within an Eccentric Horizontal Cylindrical Annulus," *Journal of Heat Transfer*, Vol. 110, No. 4, 1988, pp. 894–900.

[5] Hirose, K., Saito, F., and Ouchi, M., "Numerical Study of Natural Convection Heat Transfer in Eccentric Horizontal Cylindrical Annuli," *Transactions of the Japan Society of Mechanical Engineers*, Vol. 60, Pt. B, No. 575, 1994, pp. 2511–2517.

[6] Vaidya, N., and Shamsundar, N., "Numerical Study of Three Dimensional Natural Convection in the Eccentric Annulus Between Isothermal Horizontal Cylinders," *Heat Transfer in Microgravity Systems*, Vol. 305, American Society of Mechanical Engineers, New York, 1997, pp. 105–120.

[7] Patankar, S. V., Liu, C. H., and Sparrow, E. M., "Fully Developed Flow and Heat Transfer in Ducts Having Streamwise-Periodic Variations of Cross-Sectional Area," *Journal of Heat Transfer*, Vol. 99, No. 2, 1977, pp. 180–186.

Computations of Incompressible Flows with Natural Convection Using Pseudocompressibility Approach

J. C. Mandal,* Lokesh Agrawal,† and A. G. Marathe‡
Indian Institute of Technology, Bombay, Mumbai 400 076, India

Introduction

In recent years, there has been renewed interest in the pseudocompressibility method for computing incompressible flows due to its numerous advantages.[1] This method, originally proposed by Chorin,[2] has found its application in many areas pertaining to isothermal flows.[1,3–7] However, to our knowledge, there is no detailed investigation about the applicability of the pseudocompressibility method to heat transfer problems.

The primary difficulty in computing incompressible flows is in finding a satisfactory way to link changes in the velocity field to changes in the pressure field. This link must be accomplished to ensure the divergence-free velocity field. Among the commonly used methods for handling the velocity pressure coupling for three-dimensional problems are the pressure-based method (PBM) and the pseudocompressibility method (PCM). The basic idea in the PBM is to formulate an elliptic equation for pressure correction to update the pressure and maintain a divergence-free velocity field. The PBM, although widely used in industry, is complex computationally in the treatment of boundary conditions.[8] On the other hand, in the PCM, an artificial compressibility term is introduced in the continuity equation, which makes the system of equations strongly coupled and hyperbolic–parabolic in nature. Because of this direct coupling between the continuity and the momentum equations the PCM has been found to yield better convergence than the PBM.[8]

In the present work, the pseudocompressibility approach has been extended to compute heat transfer problems for both laminar and turbulent flow situations. A few standard natural convection test cases are evaluated to demonstrate the capability of the present formulation, namely, laminar flow in a two-dimensional differentially heated cavity,[9] a concentric annulus,[10] and a three-dimensional thermal cavity,[11] and turbulent flows inside a differentially heated cavity.[12]

Mathematical Formulation

The governing equations considered here are the time-dependent incompressible Reynolds averaged Navier–Stokes equations with the shear stress transport (SST) turbulence model,[13]

$$\frac{\partial W}{\partial t} + \frac{\partial (F^c - F^v)}{\partial x} + \frac{\partial (G^c - G^v)}{\partial y} + \frac{\partial (H^c - H^v)}{\partial z} = S$$

where

$$W = [p, u, v, w, T, k, \omega]^T$$

$$F^c = \left[\beta_{ps} u, u^2 + p + 2/3k, uv, uw, uT, uk, u\omega\right]^T$$

$$G^c = \left[\beta_{ps} v, uv, v^2 + p + 2/3k, vw, vT, vk, v\omega\right]^T$$

$$H^c = \left[\beta_{ps} w, uw, vw, w^2 + p + 2/3k, wT, wk, w\omega\right]^T$$

Presented as Paper 98-2587 at the AIAA/ASME 7th Joint Thermophysics and Heat Transfer Conference, Albuquerque, NM, 15–18 June 1998; received 25 January 2000; revision received 31 May 2000; accepted for publication 2 June 2000.

*Associate Professor, Department of Aerospace Engineering.
†Ph.D. Student, Department of Aerospace Engineering.
‡Professor, Department of Aerospace Engineering.

Table 1 Comparison of u_{max} and v_{max}

		21 × 21			41 × 41		
Velocity	*Ra*	Reference 9	Present	Deviation, %	Reference 9	Present	Deviation, %
u_{max}	10^4	16.189	15.928	1.609	16.182	16.145	0.215
v_{max}	10^4	19.197	18.911	1.490	19.509	19.485	0.120
u_{max}	10^5	36.46	36.555	0.261	35.07	35.159	0.368
v_{max}	10^5	62.79	62.359	0.685	66.73	66.997	0.401
u_{max}	10^6	79.27	74.788	5.653	67.49	68.762	1.885
v_{max}	10^6	195.44	195.369	0.036	206.32	206.586	0.129

$$F^v = \left[0,\ \tau_{11},\ \tau_{12},\ \tau_{13},\ \alpha\frac{\partial T}{\partial x},\ (\nu + \nu_t\sigma_k)\frac{\partial k}{\partial x},\ (\nu + \nu_t\sigma_w)\frac{\partial \omega}{\partial x}\right]^T$$

$$G^v = \left[0,\ \tau_{21},\ \tau_{22},\ \tau_{23},\ \alpha\frac{\partial T}{\partial y},\ (\nu + \nu_t\sigma_k)\frac{\partial k}{\partial y},\ (\nu + \nu_t\sigma_w)\frac{\partial \omega}{\partial y}\right]^T$$

$$H^v = \left[0,\ \tau_{31},\ \tau_{32},\ \tau_{33},\ \alpha\frac{\partial T}{\partial z},\ (\nu + \nu_t\sigma_k)\frac{\partial k}{\partial z},\ (\nu + \nu_t\sigma_w)\frac{\partial \omega}{\partial z}\right]^T$$

$$S = \left[0,\ 0,\ g\beta_t(T - T_0),\ 0,\ 0,\ P_k + G_k - \beta^*\omega k,\ P_w + G_w - \beta^*\omega^2 + P_{w2}\right]^T$$

$$\tau_{ij} = (\nu + \nu_t)\left(\frac{\partial u_i}{\partial x_j} + \frac{\partial u_j}{\partial x_i}\right), \qquad \alpha = \frac{\nu}{Pr} + \frac{\nu_t}{Pr_t}$$

$$Pr = \frac{C_p\mu}{K}, \qquad P_k = \nu_t\left(\frac{\partial u_i}{\partial x_j} + \frac{\partial u_j}{\partial x_i}\right)\frac{\partial u_i}{\partial x_j}$$

$$G_k = -\frac{\nu_t g_t \beta_t}{\sigma_T}\frac{\partial T}{\partial y}, \qquad P_\omega = \frac{\gamma}{\nu_t}P_k, \qquad G_\omega = \frac{\gamma C_3}{\nu_t}G_k$$

$$P_{\omega 2} = 2(1 - B_1)\sigma_{\omega 2}\frac{1}{\omega}\frac{\partial k}{\partial x_j}\frac{\partial \omega}{\partial x_j}$$

where repeated index notation implies summation over $i,\ j = 1(1)3$, x_i are the Cartesian coordinates, u_i are the corresponding velocity components, p is the pressure normalized with density, τ_{ij} is the viscous shear stress, $\boldsymbol{g}$ is the vector of gravitational acceleration, β_t is the coefficient of thermal expansion, θ is the temperature, α is the thermal diffusivity, ν is the kinematic viscosity, ν_t is the turbulent kinematic viscosity, Pr is the Prandtl number of the fluid, and Pr_T is the turbulent Prandtl number of the flow. The terms ν_t along with turbulent kinetic energy k go to zero for laminar flow. G_k and G_ω are buoyancy-related turbulence parameters, and C_3 has a value of $\tanh|v/u|$ as in Ref. 11. Here β_{ps} is an arbitrary real positive parameter representing the artificial compressibility. The optimum value of parameter β_{ps} is used as[14]

$$\beta_{ps} = k_1 \max\left[u_{ii}^2, \epsilon\right]$$

where k_1 is an arbitrary constant and ϵ is introduced to avoid ill conditioning near stagnation points and low-velocity regions. Care must be taken while choosing ϵ in natural convection problems; because the velocity field is near zero in the beginning of computations, the ϵ value decides the magnitude of β_{ps}, which is responsible for advancing the solution.

In the present study, the k–ω based SST eddy viscosity model[13] has been extended to include the buoyancy effects for heat transfer problems in a manner similar to Henkes and Hoogendoorn.[12] The SST is essentially a two-layer turbulence model that works as a k–ω model in the sublayer and logarithmic part of the boundary layer and as k–ϵ in the wake region using a blending function B_1. It has been found to perform superior to other two-equation models.[15]

Finite volume discretization has been used to solve the governing equations. The convective part of the fluxes are evaluated by taking the average of the values in the cells on either side of each face, which amounts to second-order accuracy in space. A fourth-order artificial dissipation is added to inhibit odd–even decoupling in the solution. The viscous fluxes are evaluated based on the auxiliary cell method leading to central differencing. A five-stage Runga–Kutta type of scheme is used to advance the solution in pseudotime toward steady state explicitly. A local time-stepping strategy has been used to accelerate the convergence in all of the computations.

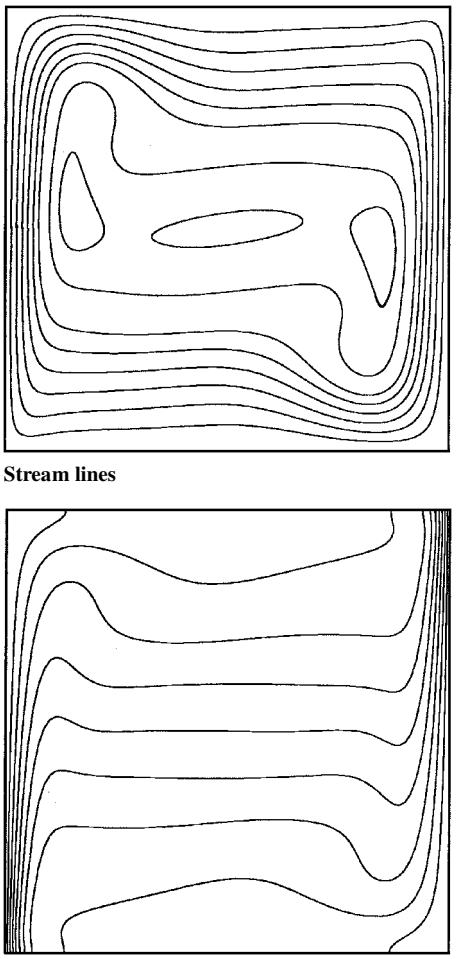

Stream lines

Temperature contours

Fig. 1 Plots for differentially heated cavity with $Ra = 10^6$.

Results and Discussions

In the present work, the pseudocompressibility formulation is extended for natural convection problems with and without turbulence. To show the applicability of the present formulation several test cases involving two- and three-dimensional thermal problems are considered and discussed next.

Laminar Results

The first problem considered is a two-dimensional flow of a Boussinesq fluid with Prandtl number 0.71 in an upright square

cavity,[9] for Rayleigh numbers Ra of 10^4, 10^5, and 10^6. The temperature at the hot wall is specified as unity and at the cold wall as zero whereas the upper and lower walls are kept adiabatic. No-slip conditions are applied at all of the walls of the cavity. Contour plots for the streamlines and the temperatures inside the cavity, for $Ra = 10^4$, 10^5, and 10^6, have been compared with the benchmark solution[9] and are found encouraging. Figure 1 shows the streamlines and temperature contours for $Ra = 10^6$. To validate the code quantitatively, values of maximum horizontal velocity u_{max} on the vertical midplane of the cavity and the values of maximum vertical velocity v_{max} on the horizontal midplane of the cavity are compared for three Rayleigh values for the uniform grid size of 21 ×21 and 41 ×41 in Table 1. From the results, it can be seen that the deviations of velocities are within 2.0% from the values given in benchmark solutions for the same grid size, except for horizontal velocity at $Ra = 10^6$ for the smaller grid size.

The second test case has been considered mainly to compute flows in non-Cartesian grids. This case involves steady natural convection flow between horizontal concentric cylinders for Boussinesq fluid.[10] The cylinders are assumed to be long; hence, the flow can be assumed two dimensional, with the inner cylinder hotter than the outer cylinder. The diameter ratio is 2.6, that is, the ratio of gap between the cylinders to the inner cylinder diameter is 0.8. The Prandtl number of the fluid is 0.706, and the Rayleigh number corresponding to the gap between the cylinders is 4.7×10^4. A body-fitted uniform grid of size 41 ×41 is employed to simulate the flow in the passage of the annulus. The temperature at the inner cylinder is specified as unity and at the outer cylinder as zero. No-slip conditions are applied at the cylindrical walls. Figure 2 shows a comparison of computed local equivalent conductivities K_{eq} at inner and outer cylinders with that of experiment[10] that matches well. The temperature profile at three different angular locations are also found to be well matched.

The third problem considered is a three-dimensional extension of two-dimensional differentially heated cavity.[11] Two opposing vertical walls are set at different temperatures, and the other walls are adiabatic. No-slip boundary conditions are applied at all of the

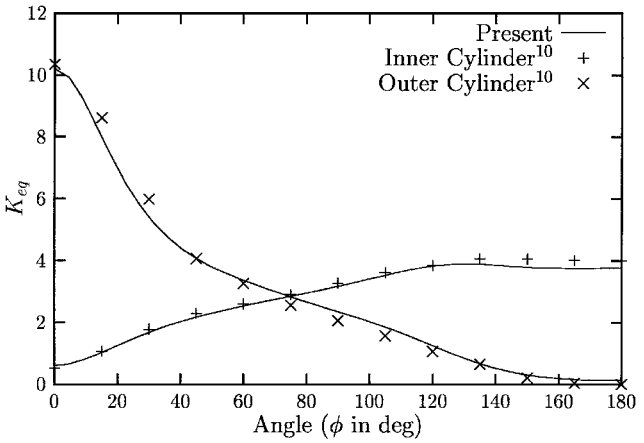

Fig. 2 Comparison of equivalent conductivity for concentric annulus.

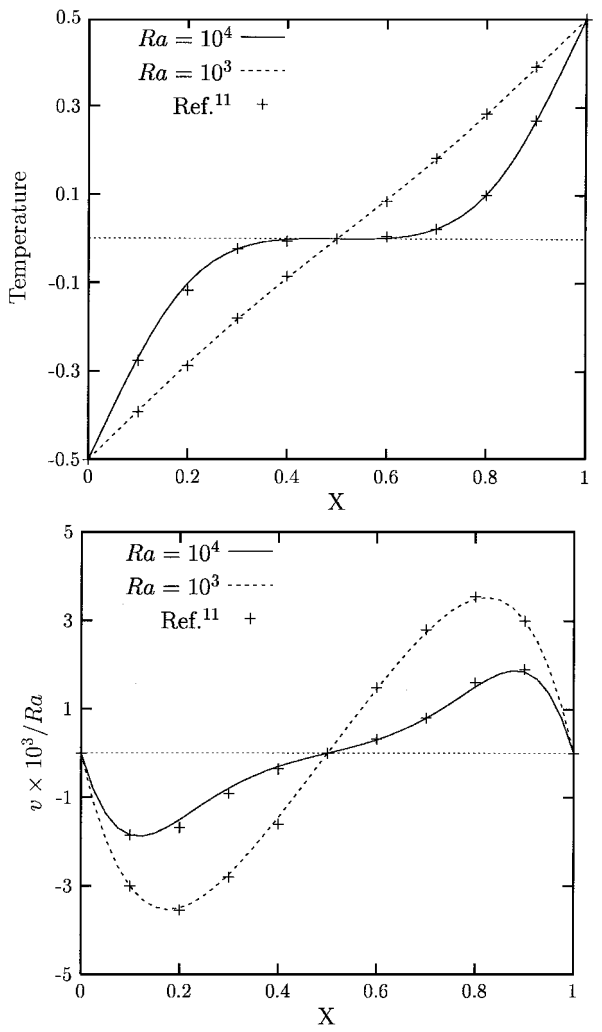

Fig. 3 Variation of temperature and vertical velocity at (x, 0.5, 0.5).

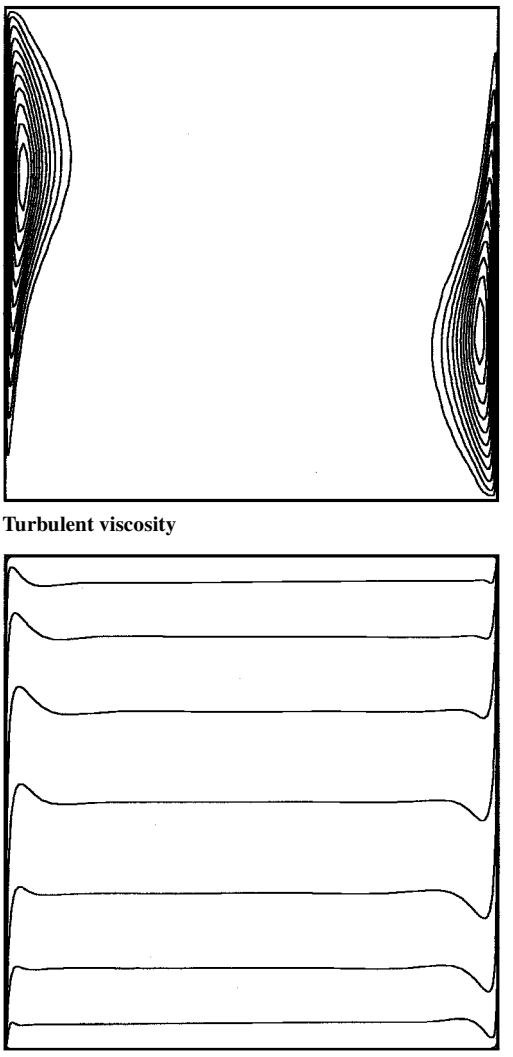

Fig. 4 Contours for differentially heated cavity with $Ra = 5 \times 10^{10}$.

walls. Because of the symmetry of the geometry and boundary conditions, only one-half of the cavity is modeled, with a grid size of $41 \times 41 \times 21$. As reported by Reddy and Reddy,[11] two test cases of Rayleigh numbers, 10^3 and 10^4, with Prandtl number equal to unity are considered here. The variation of the temperature and the vertical component of velocity vector on the horizontal midline of the symmetry plane ($y = 0.5$ and $z = 0.5$) are plotted in Fig. 3. The solutions show very good agreement with the results of Reddy and Reddy.[11]

Turbulent Results

The problem considered here is a two-dimensional square enclosure with hot left vertical wall, cold right vertical wall, and adiabatic horizontal walls. With $Pr = 0.71$ and $Ra = 5 \times 10^{10}$, the flow inside the cavity is turbulent.[12] A grid size of 57×57 with clustering (as given in Ref. 12) is used for the computations. The contour plots for temperature and turbulent kinematic viscosity are shown in Fig. 4. The present computation is able to capture the flow features such as thermal stratification in the core of the enclosure and turbulent viscosity concentration in the vertical boundary layers as given in Ref. 12. Qualitatively the contour plots agree very well with the results shown by Henkes and Hoogendoorn.[12] The quantitative comparisons of turbulent viscosity and vertical velocity along the horizontal centerline and temperature along the vertical centerline are found to be in an acceptable range of the results in Ref. 12.

Conclusions

The pseudocompressibility approach, commonly used for isothermal cases, has been successfully applied to compute flows with natural convection for both laminar and turbulent flow situations. The results obtained by the present method compare very well with experimental and benchmark numerical solutions given in the literature, thus demonstrating the ability of pseudocompressibility method in accurately predicting flows for heat transfer problems.

References

[1]Markle, C. L., and Athavale, M., "Time Accurate Unsteady Incompressible Flow Algorithms Based on Artificial Compressibility," AIAA Paper 87-1137, 1984.

[2]Chorin, A. J., "A Numerical Method for Solving Incompressible Viscous Flow Problems," *Journal of Computational Physics*, Vol. 2, No. 1, 1967, pp. 12–26.

[3]Belov, A., Martinelli, L., and Jameson, A., "A New Implicit Algorithm with Multigrid for Unsteady Incompressible Flow Calculation," AIAA Paper 95-0049, 1990.

[4]Dreyer, J., "Finite Volume Solutions to the Unsteady Incompressible Euler Equations on Unstructured Triangular Meshes," M.S. Thesis, Mechanical and Aerospace Engineering Dept., Princeton Univ., Princeton, NJ, 1990.

[5]Chang, J. L. C., Kwak, D., Rogers, S. E., and Yang, R. L., "Numerical Simulation Methods of Incompressible Flows and an Application to the Space Shuttle Main Engine," *International Journal for Numerical Methods in Fluids*, Vol. 8, 1988, pp. 1241–1266.

[6]Rizzi, A., and Eriksson, L., "Computation of Inviscid Incompressible Flow with Rotation," *Journal of Fluid Mechanics*, Vol. 153, 1985, pp. 275–312.

[7]Farmer, J., Martinelli, L., and Jameson, A., "Fast Multigrid Method for Solving Incompressible Hydrodynamic Problems with Free Surfaces," *AIAA Journal*, Vol. 32, 1994, pp. 1175–1182.

[8]Tamamidis, P., Zhang, G., and Assanis, D. N., "Comparison of Pressure Based and Artificial Compressibility Methods for Solving 3D Steady Incompressible Viscous Flows," *Journal of Computational Physics*, Vol. 124, 1996, pp. 1–13.

[9]de Vahl Devis, G., "Natural Convection of Air in a Square Cavity: A Bench Mark Numerical Solution," *International Journal for Numerical Methods in Fluids*, Vol. 3, 1983, pp. 249–264.

[10]Kuehn, T. H., and Goldstein, R. J., "An Experimental and Theoretical Study of Natural Convection in the Annulus Between Horizontal Concentric Cylinders," *Journal of Fluid Mechanics*, Vol. 74, 1976, pp. 695–719.

[11]Reddy, M. P., and Reddy, J. N., "Penalty Finite Element Analysis of Incompressible Flow Using Element by Element Solution Algorithms," *Computer Methods is Applied Mechanics and Engineering*, Vol. 100, 1992, pp. 169–205.

[12]Henkes, R. A. W. M., and Hoogendoorn, C. J., "Comparison Exercise for Computation of Turbulent Natural Convection in Enclosure," *Numerical Heat Transfer*, Pt. B, Vol. 28, 1995, pp. 59–78.

[13]Menter, F. R., "A Comparison of Some Recent Eddy-Viscosity Turbulence Models," *Journal of Fluids Engineering*, Vol. 118, 1996, pp. 514–519.

[14]Turkel, E., "Preconditioned Methods for Solving the Incompressible and Low Speed Compressible Equations," *Journal of Computational Physics*, Vol. 72, 1987, pp. 277–298.

[15]Marvin, J. G., and Huang, G. P., "Status and Future Direction for Turbulence Modeling," *Sadhana*, Vol. 23, 1998, pp. 481–503.

Freezing Couette Flow in an Annulus with Translating Outer Sleeve

Carsie A. Hall III*
University of New Orleans, New Orleans, Louisiana 70148
Calvin Mackie†
Tulane University, New Orleans, Louisiana 70118
and
Judy A. Perkins‡
North Carolina A&T State University, Greensboro, North Carolina 27411

Introduction

INTERNAL fluid flows undergoing phase change (melting or freezing) have been the subject of research due to applications in manufacturing processes, freeze blockage of liquids in pipes, low-temperature viscometers, circular and annular thrust bearings, etc.[1,2] Typically, these fluids exhibit Newtonian as well as non-Newtonian behavior.[3,4] Analytical solutions to flows that exhibit Couette (or Couette-like) behavior such as purely shear-driven flows and near-wall turbulent flows with solid–liquid phase change have appeared sparsely in the literature. Most analytical solutions have been obtained for problems involving semi-infinite regions. For example, Huang[5] studied the transient Couette flow problem with viscous heating and used a combination of the similarity technique and Green's function to derive a closed-form solution for one-dimensional melting of a semi-infinite solid region by a hot moving wall.

In the present Note, an analytical solution is presented for one-dimensional freezing of laminar, fully developed Couette flow within an annular region with viscous dissipation. The solution is valid for small (at least an order of magnitude less than unity) but nonvanishing Stefan numbers. A translating outer sleeve induces the shear-driven motion in the liquid region. A closed-form expression for the instantaneous location of the solid–liquid interface is derived. In addition, expressions for the Nusselt number at the solid–liquid interface and dimensionless power (per unit length) are all derived as a function of pertinent dimensionless parameters. The analytical solution reduces to a few classical results in the appropriate asymptotic limits.

Problem Formulation

Shown in Fig. 1 is a one-dimensional region of thickness $(R_o - R_i)$. The motion of the liquid in the annular region, assumed to be laminar and fully developed, is shear driven by an outer cylinder or sleeve moving at constant speed V. The outer sleeve is modeled as

Received 24 December 1999; revision received 11 April 2000; accepted for publication 13 April 2000.

*Assistant Professor, Department of Mechanical Engineering; cahall@uno.edu. Member AIAA.

†Assistant Professor, Department of Mechanical Engineering.

‡Associate Professor, Department of Civil and Environmental Engineering.